Pairing anisotropy and macroscopic anisotropy of superconductors

Yuji Suwa* and Masaru Tsukada
Department of Physics, University of Tokyo, Bunkyo-ku, Tokyo 113, Japan
(Received 30 May 1989)

Macroscopic properties of the superconductivity are investigated in the tight-binding picture taking account of the intersite pairing as well as the on-site pairing. We discuss the case of a layered material, a cubic material, and a quasi-one-dimensional material. A multicomponent Ginzburg-Landau equation, which takes the intersite-pairing effect into account as the different components of the order parameter, is derived from a microscopic theory. The angle dependence of the upper-critical field H_{c2} is analyzed based on that equation and how the intersite interactions affect the anisotropy of H_{c2} is clarified. The Fermi-energy dependence of the transition temperature T_c, which does not simply reflect the density of states, is also discussed.

I. INTRODUCTION

Recently discovered high-T_c oxide superconductors have attracted much attention. A number of theoretical models have been proposed and many kinds of nonphonon mechanisms have been suggested to explain the high-temperature superconductivity. They agree on the point that their electronic systems are strongly correlated. This means that two electrons feel a strong Coulomb repulsion when they approach each other. However, there must be an attractive interaction between the electrons in a superconductor. When one describes the electronic system in the tight-binding picture, this situation can be expressed by the attractive intersite interaction, which acts between the two electrons at different sites, and repulsive or weakly attractive on-site interaction, which acts between the two at the same site.

The tight-binding model would be more suitable to describe the electronic structure of the high-T_c materials than the free-electron model, since their band widths are considered to be narrow. A distinctive feature of the high-T_c materials is that the interelectron interaction is of short range, and thus the discreteness of the lattice would crucially reflect on the superconducting properties. A similar situation holds for the heavy-fermion superconductors that have very narrow band widths. To fully understand the properties of these superconductors, it is important to clarify the effect of the discreteness of the lattice on the properties of the superconductivity. For that purpose, the tight-binding picture (lattice model) is the most appropriate one and the usual free-electron picture (continuum model) cannot be used.

For the discussion of the spatial variation of the order parameter, the real-space representation has often been employed. In those theories formulated in the continuum model, the attractive interaction is supposed to act only between the two electrons on the same point (we call it continuum point interaction model). When one transfers this point-interaction model to the lattice model, it is necessary to determine the size of the interacting point. The easiest way is to take account only of the on-site interaction, neglecting the intersite interactions. However, there might be cases where the intersite interaction brings about a qualitatively different feature compared to the system with the on-site interaction alone. One purpose of this paper is to clarify this problem by treating the intersite interaction on equal footing with the on-site interaction.

Our approach to this problem is to investigate the anisotropy of the superconductor. The word "anisotropy" is used in two different ways in general. One is the pairing anisotropy and the other is the macroscopic anisotropy, i.e., the anisotropy of macroscopic properties such as H_{c2}. The general form of the order parameter for superconductivity can be written as

$$\langle \psi^\dagger(\mathbf{r})\psi^\dagger(\mathbf{r}')\rangle = \Delta^*(\mathbf{r},\mathbf{r}') = \Delta^*[\mathbf{r}-\mathbf{r}';\tfrac{1}{2}(\mathbf{r}+\mathbf{r}')] ,$$

where $\psi^\dagger(\mathbf{r})$ is the creation operator of the electron on the point $\mathbf{r}$. Pairing anisotropy can be discussed using the relative coordinate dependence of the order parameter neglecting the center-of-mass coordinate. On the other hand, macroscopic anisotropy is related to the center-of-mass coordinate. So, existing theories of the point-interaction model treat the macroscopic properties, neglecting the relative coordinate. However, the relative coordinate dependence on the order parameter may affect the macroscopic property.

When one describes the macroscopic properties of a superconductor near the transition temperature, the Ginzburg-Landau (GL) equation affords an effective method. However, the derivation of the GL equation is based on the point-interaction continuum model. Therefore, the usual GL equation treats only the center-of-mass coordinate dependence of the order parameter. To describe the effect of the anisotropy pertinent to the internal structure of the electron pair, it is necessary to include the freedom of the relative coordinate in the GL equation. We are developing a multicomponent GL equation in the lattice model that includes the essential parts of the relative coordinate as well as the center-of-mass coordinate. Using that equation, we discuss how the on-site and intersite interaction play their roles in su-

perconductivity and give a qualitative picture of the dependence of the macroscopic properties on the anisotropic pairing.

In our previous paper[1] we have investigated the interlayer pairing, which is the simplest example of the intersite pairing. There a two-component GL equation, which takes account of the intralayer and interlayer pairings, was derived, and the macroscopic anisotropy induced by the interlayer pairing was discussed. A part of the results will be seen again later.

Our purpose here is to investigate more general types of intersite pairings for the various types of materials. We also aim to include the possibility of spin triplet pairing, which was not included in the previous paper. There are various internal structures of the pairing state corresponding to s-, p-, d-, . . . symmetry states; states other than the s-wave symmetry state are usually called anisotropic pairing states. The internal structure of the pair is determined by the following factors: (1) the relative magnitude of the on-site and various intersite-pairing interactions, (2) the energy band and the Fermi surface of the single-electron state, and (3) the external field. It is very important to have a perspective view about how the internal structure of the pair is determined by the competition among the above-mentioned factors. To investigate this problem using a unified viewpoint, we choose the simple tight-binding system and discuss the three types of materials listed in the following: (1) layered systems with tetragonal symmetry, (2) cubic system, and (3) quasi-one-dimensional systems with tetragonal symmetry.

For the layered system, one possibility for intersite pairing is the interlayer coupling, which corresponds to the intersite interaction in the direction perpendicular to the layer. Several authors[2,3] have discussed the relative stability of the phase with the interlayer pairing and that with the intralayer pairing. Gulácsi *et al.*[3] concluded that the mixing effect of the interlayer and intralayer pairing raises the transition temperature. In our previous paper, we pointed out that the mixing effect is very weak for the free-electron band. One can expect, however, an appreciable mixing for the energy bands with sharp structures at the density of states (DOS).

The other type of the intersite interaction in the layered system is the intralayer intersite interaction that acts between the two electrons at different sites in the same layer. Recently, several authors have suggested this type of pairing interaction as the origin of high-T_c superconductivity. For example, Kamimura *et al.*[4] proposed a spin-polaron model where attractive interaction acts between two electrons at the nearest-neighbor sites. Our model systems treated here mimic such a layered superconductor and should reveal some important characteristics.

For the heavy-fermion superconductors, the possibility of the anisotropic (non-s-wave) pairing is studied by many authors.[5-7] Miyake *et al.*[6] proposed a cubic lattice model with on-site and intersite interaction. They estimated the intersite coupling constant and obtained the result that d pairing is favorable in a certain parameter region. However, they investigated systematically neither how the appearance of the d-pairing state is determined by the band filling, nor how H_{c2} is influenced by the anisotropic pairing. In this paper we will study how the anisotropy of H_{c2} reflects the internal structure of the pair in such a system. Besides the discussion of H_{c2}, we will also discuss T_c from the view of the electron number dependence in which the character of the intersite pairing is reflected. We will show that the s pairing is preferable when the band filling by the carrier is little, while d pairing is preferable when the band is nearly half filled as in the case of the singlet pairing.

Quasi-one-dimensional superconductors,[8,9] such as $(SN)_x$ or organic superconductors, show very anisotropic properties. Our model, by choosing appropriate values for parameters, can describe such quasi-one-dimensional superconductors. We pay special attention to the two kinds of intersite interactions, the interchain interaction,[10] and the intrachain intersite interaction.

The plan of this paper is as follows. In Sec. II, the tight-binding model is introduced and the types of possible pairing states are classified. In Sec. III, the linearized equation for the order parameter is derived for the uniform system. Transition temperature is discussed based on this linearized equation. The multicomponent GL equation is obtained from the microscopic model in Sec. IV. In Sec. V, the upper-critical field H_{c2} is obtained from the GL equation and the influence of the pair internal structure on the anisotropy of H_{c2} is clarified. In this paper we use $c=\hbar=k_B=1$.

II. MODEL AND CLASSIFICATION OF THE PAIRING STATES

In the model treated in this paper, sites are arranged on the orthorhombic lattice with the lattice constants, S_x, S_y, and S_z. We assume that there are transfer integrals only between the nearest neighbors in each direction; they are denoted as t_x, t_y, and t_z. To simplify the model we include only the nearest-neighbor intersite interactions, V_x, V_y, and V_z, as well as the on-site interaction, V_0. Though we do not discuss the origin of the pairing interaction, it would not be unreasonable to assume quite localized interactions as in this model.

The Hamiltonian is thus written as

$$H=\sum_{\sigma}\sum_{\mathbf{j}}\left[-\sum_{l}\frac{t_l}{2}\psi_\sigma^\dagger(\mathbf{j})\psi_\sigma(\mathbf{j}+\boldsymbol{l})-\mu\psi_\sigma^\dagger(\mathbf{j})\psi_\sigma(\mathbf{j})-\sum_{\sigma'}\sum_{l}\left[\frac{V_l^0}{2}\psi_\sigma^\dagger(\mathbf{j})\psi_{\sigma'}^\dagger(\mathbf{j}+\boldsymbol{l})\psi_{\sigma'}(\mathbf{j}+\boldsymbol{l})\psi_\sigma(\mathbf{j})+\frac{V_l^1}{2}\psi_\sigma^\dagger(\mathbf{j})\psi_{\sigma'}^\dagger(\mathbf{j}+\boldsymbol{l})\psi_{\sigma'}(\mathbf{j})\psi_\sigma(\mathbf{j}+\boldsymbol{l})\right]\right], \tag{1}$$

where the summation $\sum_l$ is taken over the center site and all its nearest neighbors: $l=0,\pm S_x\mathbf{e}_x,\pm S_y\mathbf{e}_y,\pm S_z\mathbf{e}_z$ ($\mathbf{e}_x,\mathbf{e}_y,\mathbf{e}_z$ are the unit vectors directed to each axis). $\mathbf{j}$ represents the position of a site and σ represents the spin of the electron. V_l^0 and V_l^1 represent the direct and exchange type inter-electron potential, respectively. Without losing the generality, we can assume $V_l^i=V_{-l}^i$. We introduced the notations of t_l as $t_{\pm S_x\mathbf{e}_x}=t_x, t_{\pm S_y\mathbf{e}_y}=t_y, t_{\pm S_z\mathbf{e}_z}=t_z$ and $t_0=0$.

This Hamiltonian can be used as the layered materials, cubic materials, and quasi-one-dimensional materials according to the ratio of the transfer integral. By setting various combination of the pairing interactions, different types of the ordered states are realized. The types of the ordered states we investigated are listed in Table I, II, and III.

The dependence of the order parameters on the relative coordinates of the electron pair is represented by the presence of the four components of the order parameter: $\Delta_0,\Delta_x,\Delta_y,\Delta_z$, which are defined by

$$\Delta_\ell=\Delta\left[l;\frac{\mathbf{r}+\mathbf{r}'}{2}\right] \tag{2}$$

with $\ell=0,x,y,z$ corresponding to $l=0,S_x\mathbf{e}_x,S_y\mathbf{e}_y,S_z\mathbf{e}_z$. Rigorously speaking, we should distinguish the spin singlet pairing and the spin triplet pairing components as will be discussed later [see Eqs. (15) and (16)]. Other components of Δ_ℓ corresponding to more distant sites vanish, because the pairing interaction in our model does not extend beyond the nearest neighbors.

III. TRANSITION TEMPERATURE FOR THE UNIFORM SYSTEM

Before the discussion of the macroscopic anisotropy induced by the anisotropic pairing, we discuss the stability of the ordered states by studying the transition temperature. For that purpose, we derive a linearized equation for the uniform system.

The Green's functions, G and F, are introduced by the standard definition as in our previous paper:[1]

$$G_\sigma(\mathbf{j},\mathbf{j}',\tau-\tau')\equiv-\langle T_\tau\psi_\sigma(\mathbf{j},\tau)\psi_\sigma^\dagger(\mathbf{j}',\tau')\rangle\ , \tag{3}$$

$$F_{\sigma\sigma'}^\dagger(\mathbf{j},\mathbf{j}',\tau-\tau')\equiv-\langle T_\tau\psi_\sigma^\dagger(\mathbf{j},\tau)\psi_{\sigma'}^\dagger(\mathbf{j}',\tau')\rangle\ . \tag{4}$$

The self-energies and the order parameters are defined as

$$Z_\sigma^i(\mathbf{j},\mathbf{j}+l)\equiv V_l^iG_\sigma(\mathbf{j},\mathbf{j}+l,\tau=0)\ , \tag{5}$$

$$\Delta_{\sigma\sigma'}^0(\mathbf{j},\mathbf{j}+l)\equiv V_l^0F_{\sigma\sigma'}(\mathbf{j},\mathbf{j}+l,\tau=0)\ , \tag{6}$$

$$\Delta_{\sigma\sigma'}^1(\mathbf{j},\mathbf{j}+l)\equiv V_l^1F_{\sigma\sigma'}(\mathbf{j}+l,\mathbf{j},\tau=0)\ . \tag{7}$$

Using these order parameters, self-energies, and the Fourier transforms of the Green's functions with respect to τ, we get two equations by the standard procedure of the mean-field theory,

$$\left[i\omega_n+\mu+\sum_l\left[\sum_{\sigma'}Z_{\sigma'}^0(\mathbf{j}+l,\mathbf{j}+l)-Z_\sigma^1(\mathbf{j}+l,\mathbf{j}+l)\right]\right]G_\sigma(\mathbf{j},\mathbf{j}',\omega_n)$$
$$+\sum_l\left[\frac{t_l}{2}-Z_\sigma^0(\mathbf{j},\mathbf{j}+l)+\sum_{\sigma'}Z_{\sigma'}^1(\mathbf{j},\mathbf{j}+l)\right]G_\sigma(\mathbf{j}+l,\mathbf{j}',\omega_n)-\sum_l\sum_{\sigma'}\sum_i\Delta_{\sigma\sigma'}^i(\mathbf{j},\mathbf{j}+l)F_{\sigma'\sigma}^\dagger(\mathbf{j}+l,\mathbf{j}',\omega_n)=\delta_{\mathbf{j}\mathbf{j}'}\ , \tag{8}$$

$$\left[i\omega_n-\mu-\sum_l\left[\sum_{\sigma''}Z_{\sigma''}^0(\mathbf{j}+l,\mathbf{j}+l)-Z_\sigma^1(\mathbf{j}+l,\mathbf{j}+l)\right]\right]F_{\sigma\sigma'}^\dagger(\mathbf{j},\mathbf{j}',\omega_n)$$
$$-\sum_l\left[\frac{t_l}{2}-Z_\sigma^0(\mathbf{j}+l,\mathbf{j})+\sum_{\sigma''}Z_{\sigma''}^1(\mathbf{j}+l,\mathbf{j})\right]F_{\sigma\sigma'}^\dagger(\mathbf{j}+l,\mathbf{j}',\omega_n)+\sum_l\sum_i\Delta_{\sigma\sigma'}^{*i}(\mathbf{j},\mathbf{j}+l)G_{\sigma'}(\mathbf{j}+l,\mathbf{j}',\omega_n)=0\ , \tag{9}$$

where ω_n is a Matsubara frequency. Using the normal-state Green's functions G_σ^{00} and neglecting the self-energies Z_σ^i, we obtain

$$G_\sigma(\mathbf{j},\mathbf{j}',\omega_n)=G_\sigma^{00}(\mathbf{j},\mathbf{j}',\omega_n)+\sum_{\mathbf{j}_1}\sum_{l_1}\sum_{\sigma''}\sum_iG_\sigma^{00}(\mathbf{j},\mathbf{j}_1,\omega_n)\Delta_{\sigma\sigma''}^i(\mathbf{j}_1,\mathbf{j}_1+l_1)F_{\sigma''\sigma}^\dagger(\mathbf{j}_1+l_1,\mathbf{j}',\omega_n)\ , \tag{10}$$

$$F_{\sigma\sigma'}^\dagger(\mathbf{j},\mathbf{j}',\omega_n)=\sum_{\mathbf{j}_1}\sum_{l_1}\sum_iG_\sigma^{00}(\mathbf{j}_1,\mathbf{j},-\omega_n)\Delta_{\sigma\sigma'}^{*i}(\mathbf{j}_1,\mathbf{j}_1+l_1)G_{\sigma'}(\mathbf{j}_1+l_1,\mathbf{j}',\omega_n)\ . \tag{11}$$

Under the condition that the order parameters are small enough, we can approximate $G_{\sigma'}$ in the right-hand side of Eq. (11) by the normal-state Green's function $G_{\sigma'}^{00}$. Then we obtain

$$\Delta_{\sigma\sigma'}^{*0}(\mathbf{j},\mathbf{j}+l)/V_l^0=-\Delta_{\sigma'\sigma}^{*1}(\mathbf{j},\mathbf{j}+l)/V_l^1$$
$$=\sum_{\omega_n}\sum_{\mathbf{j}_1}\sum_{l_1}\sum_{i_1}G_\sigma^{00}(\mathbf{j}_1,\mathbf{j},-\omega_n)\Delta_{\sigma\sigma'}^{*i_1}(\mathbf{j}_1,\mathbf{j}_1+l_1)G_{\sigma'}^{00}(\mathbf{j}_1+l_1,\mathbf{j}+l,\omega_n)\ . \tag{12}$$

It is convenient to use the new parameters defined as

$$V_{\ell}^{s} \equiv V_{l}^{0} + V_{l}^{1} , \tag{13}$$

$$V_{\ell}^{t} \equiv V_{l}^{0} - V_{l}^{1} , \tag{14}$$

$$\Delta_{\ell}^{s} \equiv V_{\ell}^{s} \sum_{\omega_n} [F_{\sigma-\sigma}(\mathbf{j},\mathbf{j}+\boldsymbol{l},\omega_n) - F_{-\sigma\sigma}(\mathbf{j},\mathbf{j}+\boldsymbol{l},\omega_n)] , \tag{15}$$

$$\Delta_{\ell\sigma\sigma'}^{t} \equiv V_{\ell}^{t} \sum_{\omega_n} [F_{\sigma\sigma'}(\mathbf{j},\mathbf{j}+\boldsymbol{l},\omega_n) + F_{\sigma'\sigma}(\mathbf{j},\mathbf{j}+\boldsymbol{l},\omega_n)] . \tag{16}$$

Δ_{ℓ}^{s}'s and Δ_{ℓ}^{t}'s are the quantities corresponding to those defined by Eq. (2). When the dependence of these quantities on the center-of-mass coordinate j is evident, we omitted writing it explicitly. Later, we will express the spin triplet order parameters as

$$\Delta_{\ell\uparrow\downarrow}^{t} \rightarrow \Delta_{\ell}^{0},\ \Delta_{\ell\uparrow\uparrow}^{t} \rightarrow \Delta_{\ell}^{+1},\ \Delta_{\ell\downarrow\downarrow}^{t} \rightarrow \Delta_{\ell}^{-1} , \tag{17}$$

but here we simply denote Δ_{ℓ}^{t} as any one of them.

After some straightforward calculations, the self-consistent equation of Δ is obtained as follows:

$$\Delta_{\ell}^{\nu *} / V_{\ell}^{\nu} = \sum_{\ell'} {}^{\nu}K_{\ell\ell'} \Delta_{\ell'}^{\nu *} , \tag{18}$$

where, $\nu = s,t$ and the summation $\sum_{\ell'}$ is taken over $\ell' = 0,x,y,z$. The coefficient, ${}^{\nu}K_{\ell\ell'}$, is defined as

$${}^{\nu}K_{\ell\ell'} = \frac{S_x S_y S_z T}{2(2\pi)^3} \sum_{\omega_n} \int d\mathbf{k} \frac{(e^{i\mathbf{k}\cdot\boldsymbol{l}} \pm e^{-i\mathbf{k}\cdot\boldsymbol{l}})(e^{-i\mathbf{k}\cdot\boldsymbol{l}'} \pm e^{i\mathbf{k}\cdot\boldsymbol{l}'})}{\omega_n^2 + \varepsilon_{\mathbf{k}}^2} , \tag{19}$$

where + is for $\nu = s$, − is for $\nu = t$, and

$$\varepsilon_{\mathbf{k}} = -\sum_{X} t_X \cos(k_X S_X) - \mu . \tag{20}$$

In the preceding equations, $\varepsilon_{\mathbf{k}}$ is a three-dimensional energy dispersion and T is the temperature. The summation $\sum_X$ is taken over $X = x,y,z$.

To see the effects of the form factor

$$(e^{i\mathbf{k}\cdot\boldsymbol{l}} \pm e^{-i\mathbf{k}\cdot\boldsymbol{l}})(e^{-i\mathbf{k}\cdot\boldsymbol{l}'} \pm e^{i\mathbf{k}\cdot\boldsymbol{l}'})$$

of the pair on the transition temperature, we approximate ${}^{\nu}K_{\ell\ell'}$'s of Eq. (19) as

$${}^{\nu}K_{\ell\ell'} \approx N_{\ell\ell'}^{\nu} \ln\left[\frac{1.13\omega_D}{T}\right] , \tag{21}$$

where

$$N_{\ell\ell'}^{\nu} \equiv \tfrac{1}{2} \sum_{\mathbf{k}} \delta(\varepsilon_{\mathbf{k}})(e^{i\mathbf{k}\cdot\boldsymbol{l}} \pm e^{-i\mathbf{k}\cdot\boldsymbol{l}})(e^{-i\mathbf{k}\cdot\boldsymbol{l}'} \pm e^{i\mathbf{k}\cdot\boldsymbol{l}'}) . \tag{22}$$

This approximation is justified by the fact that the contribution to the $\mathbf{k}$ integral in Eq. (19) is dominantly from the region of $\varepsilon_{\mathbf{k}} \sim 0$. The quantity $N_{\ell\ell'}^{\nu}$ includes all the information of the pair structure and the single-electron energy bands. In particular, the diagonal element represents the DOS of the band weighted by the form factor. From Eqs. (18) and (21), the eigenvalue equation can be derived as

$$\begin{bmatrix} \Lambda^s & 0 \\ 0 & \Lambda^t \end{bmatrix} \begin{bmatrix} \Delta^s \\ \Delta^t \end{bmatrix} = \frac{1}{\ln\left[\dfrac{1.13\omega_D}{T}\right]} \begin{bmatrix} I_4 & 0 \\ 0 & I_3 \end{bmatrix} \begin{bmatrix} \Delta^s \\ \Delta^t \end{bmatrix} , \tag{23}$$

where Λ^s and Λ^t are 4×4 and 3×3 matrices, respectively, whose $\ell\ell'$ elements are

$$\Lambda_{\ell\ell'}^{\nu} \equiv N_{\ell\ell'}^{\nu} V_{\ell}^{\nu} . \tag{24}$$

The row and column corresponding to $\ell = 0$ or $\ell' = 0$ are absent for Λ^t. I_4 and I_3 are 4×4 and 3×3 unit matrices, respectively. We should diagonalize only Λ^s, since Λ^t has no off-diagonal elements.

In terms of the maximum eigenvalue, $\lambda_{\max}$, of the matrix in the left-hand side of Eq. (23), the transition temperature is expressed as

$$T_c = 1.13\omega_D \exp\left[-\frac{1}{\lambda_{\max}}\right] . \tag{25}$$

The eigenvector that corresponds to $\lambda_{\max}$ represents the internal structure of the pair wave function.

A. Layered material with intralayer and interlayer pairing

First we analyze the system with interlayer coupling V_z^{ν} ($\nu = s,t$) and intralayer coupling V_0^s. When we set $V_x^{\nu} = V_y^{\nu} = 0$, Eq. (18) can be reduced to 2×2 secular equation for Δ_z^s and Δ_0^s for the singlet case, and a scalar equation for Δ_z^t for the triplet case. $\lambda_{\max}$, which determines T_c by Eq. (25), is the larger of

$$\lambda^s = \tfrac{1}{2}\{ V_z^s N_{zz}^s + V_0^s N_{00}^s + [(V_z^s N_{zz}^s - V_0^s N_{00}^s)^2 + 4V_0^s V_z^s N_{0z}^{s2}]^{1/2} \} , \tag{26}$$

$$\lambda^t = V_z^t N_{zz}^t , \tag{27}$$

where $N_{0z}^s = N_{z0}^s$.

In the following, we investigate the behavior of T_c as the function of the chemical potential numerically. The origin of the chemical potential is chosen as the band center. We choose the case of $t_x = t_y = 10t_z$, as a typical example of the layered system. Figure 1 shows the μ dependence of T_c for various cases. The case of singlet pairing in the presence of the intralayer and interlayer couplings is shown in Fig. 1(a). Though this is the same case as in our previous paper,[1] we again discuss this case briefly. $V_z^s = V$ is assumed in all lines. The μ dependence of the dashed line ($V_0^s = V$) more or less reflects the DOS of the single-electron state. However, with the decrease of the on-site interaction V_0^s, the dip of T_c at the band center ($\mu \sim 0$) is enhanced. Thus the μ dependence of the solid line ($V_0^s = 0$) corresponding to the case of the interlayer coupling alone is considerably different from the dashed line. The enhancement of the dip at $\mu \sim 0$ originates from the characteristic μ dependence of N_{zz}^s and

N^s_{00} as discussed in the previous paper. It is remarkable that the dotted line ($V^s_0=-\frac{1}{2}V$) is nearly the same as the solid line ($V^s_0=0$). This suggests that when the interlayer pairing dominates, T_c is not so suppressed by the repulsive on-site interaction.

The critical temperature T_c for the triplet interlayer state is determined by Eq. (25) with $\lambda_{\max}=\lambda^t$. Figure 1(b) shows the μ dependence of T_c for the triplet state for the case of $V^t_z=V$, $V^t_x=V^t_y=0$. For the triplet case, the cusp points seen in the case of the singlet pairing [Fig. 1(a)] are rounded off. A rounded shape of the T_c versus μ curve is common to the various cases of the triplet pairing, as will be seen later.

B. Layered material with onsite and intralayer intersite pairing

Next we discuss the effect of the intralayer intersite interaction $V^v_x=V^v_y$ neglecting the interlayer coupling, $V^v_z=0$. The onsite interaction V^s_0 coexists for the case of the singlet pairing, but does not exist for the case of the triplet pairing. Then, Eq. (18) can be reduced to 3×3 secular equation for Δ^s_x, Δ^s_y, and Δ^s_0 for the singlet pairing, and 2×2 secular equation for Δ^t_x and Δ^t_y for the triplet pairing. $\lambda_{\max}$ is the largest one of

$$\lambda^s_s=\tfrac{1}{2}\{(N^s_{xy}+N^s_{xx})V^s_x+N^s_{00}V^s_0+\{[(N^s_{xy}+N^s_{xx})V^s_x-N^s_{00}V^s_0]^2+8N^{s2}_{0x}V^s_0V^s_x\}^{1/2}\}, \tag{28}$$

$$\lambda^s_d=(N^s_{xx}-N^s_{xy})V^s_x, \tag{29}$$

$$\lambda^t=N^t_{xx}V^t_x. \tag{30}$$

λ^s_s corresponds to the s-wave state, while λ^s_d corresponds to the d-wave state [see Table I].

Figure 1(c) shows the μ dependence of T_c for the case of the singlet pairing in the presence of the intralayer in-

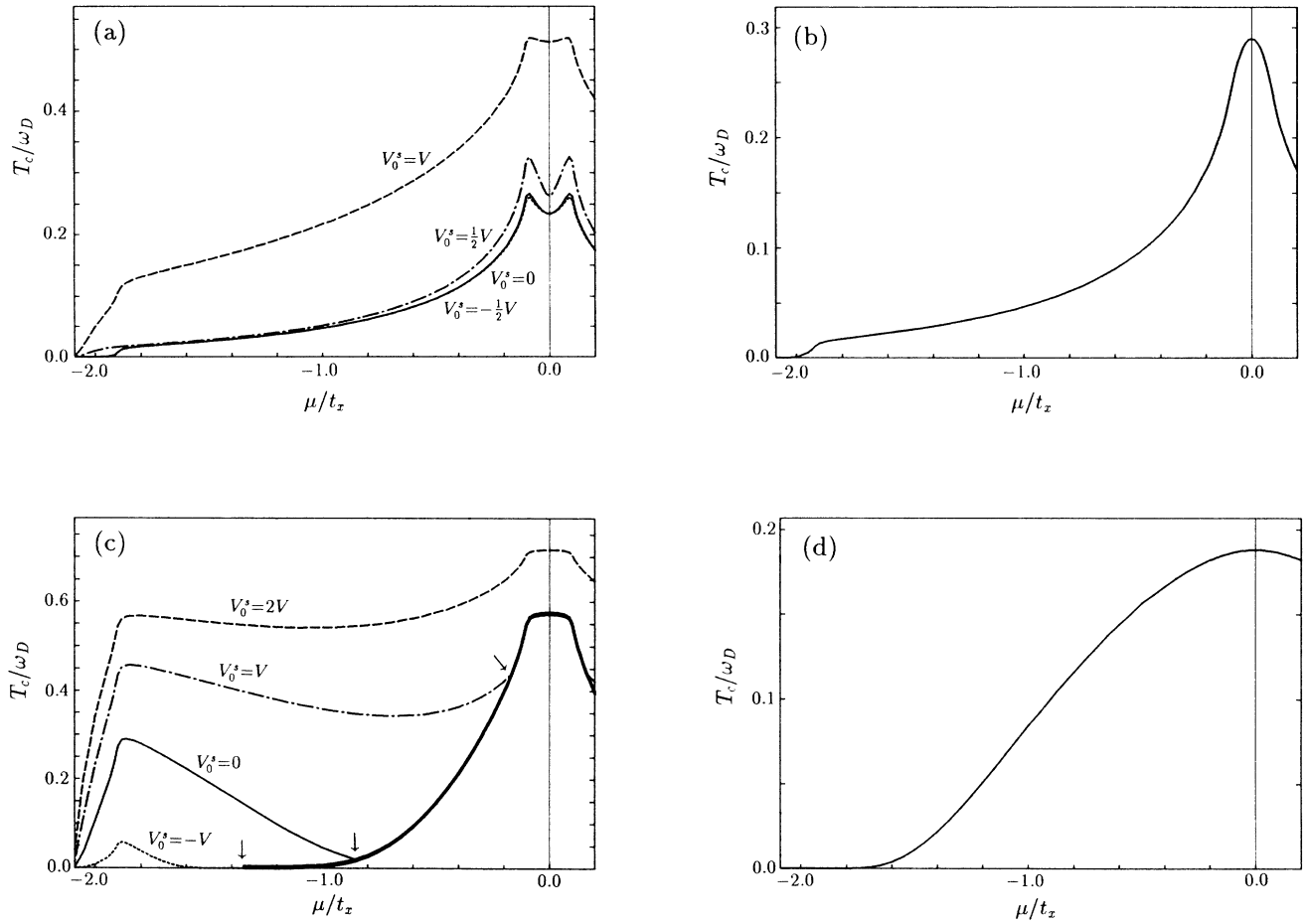

FIG. 1. T_c vs μ for the layered system ($10t_z=t_x=t_y$). The origin of μ is chosen at the band center. (a) The case of singlet pairing in the presence of the intralayer and interlayer coupling, $V^s_z=V$, $V^s_x=V^s_y=0$. (b) The case of triplet pairing in the presence of the interlayer coupling, $V^t_z=V$, $V^t_x=V^t_y=0$. (c) The case of singlet pairing in the presence of the intralayer intersite interaction, $V^s_x=V^s_y=V$, $V^s_z=0$. The bold line represents the region of the d-symmetry state. Others correspond to the s-symmetry states. (d) The case of triplet pairing in the presence of the intralayer intersite interaction, $V^t_z=0$, $V^t_x=V^t_y=V$.

tersite interaction. $V_x^s=V_y^s=V$, $V_z^s=0$ is assumed for all lines. In the dashed line ($V_0^s=2V$), the order parameter has s-wave symmetry. When the on-site interaction is reduced, the order parameter has d-wave symmetry in the region near $\mu=0$. The d-symmetry region is represented by the thick line. The position marked by arrow in each line ($V_0^s=V,0,-V$) represents the boundary between the s-wave and d-wave symmetry region. In the region of the d-wave symmetry, T_c does not depend on the value of V_0^s, because it is determined by Eq. (25) and (29) which does not include V_0^s. On the other hand, repulsive V_0^s diminishes T_c for the s-wave state.

Figure 1(d) shows the μ dependence of T_c for the triplet pairing in the presence of the intralayer intersite interaction i.e., $V_z^t=0$, $V_x^t=V_g^t=V$. The curve of T_c versus μ is of smooth bell type and does not reflect the structure of DOS. This feature is quite different from other cases [Figs. 1(a)~1(c)].

Even for general cases of the triplet pairing, $V_z^t\neq 0$, $V_x^t=V_y^t\neq 0$, the two types of pairing Δ_x^t and Δ_z^t never coexist, i.e., either Δ_x^t or Δ_z^t should vanish. This is because the matrix Λ^t has no off-diagonal elements as seen

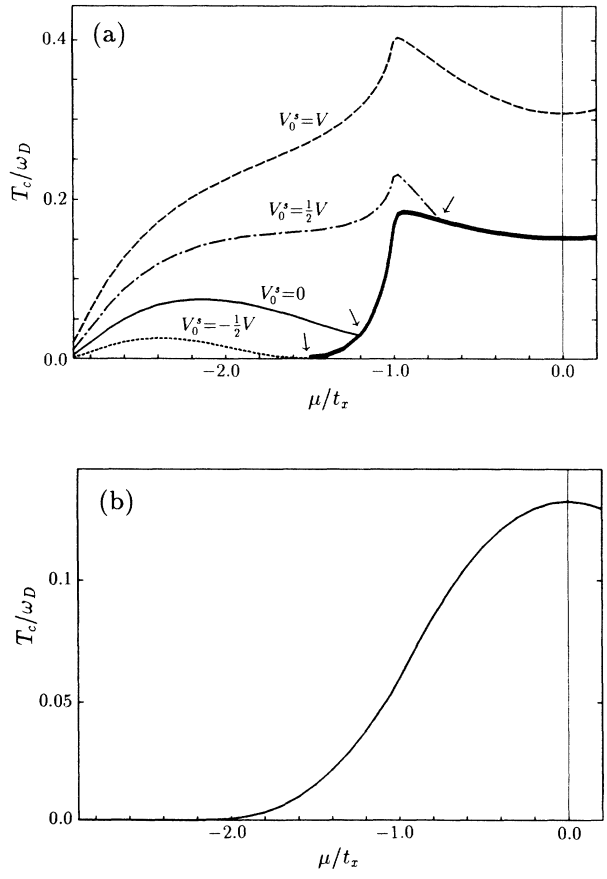

FIG. 2. T_c vs μ for the cubic system ($t_x=t_y=t_z$). (a) The case of singlet pairing in the presence of the on-site and intersite interactions, $V_x^s=V_y^s=V_z^s=V$. The bold line represents the d-symmetry region. (b) The case of triplet pairing in the cubic system, $V_x^t=V_y^t=V_z^t=V$.

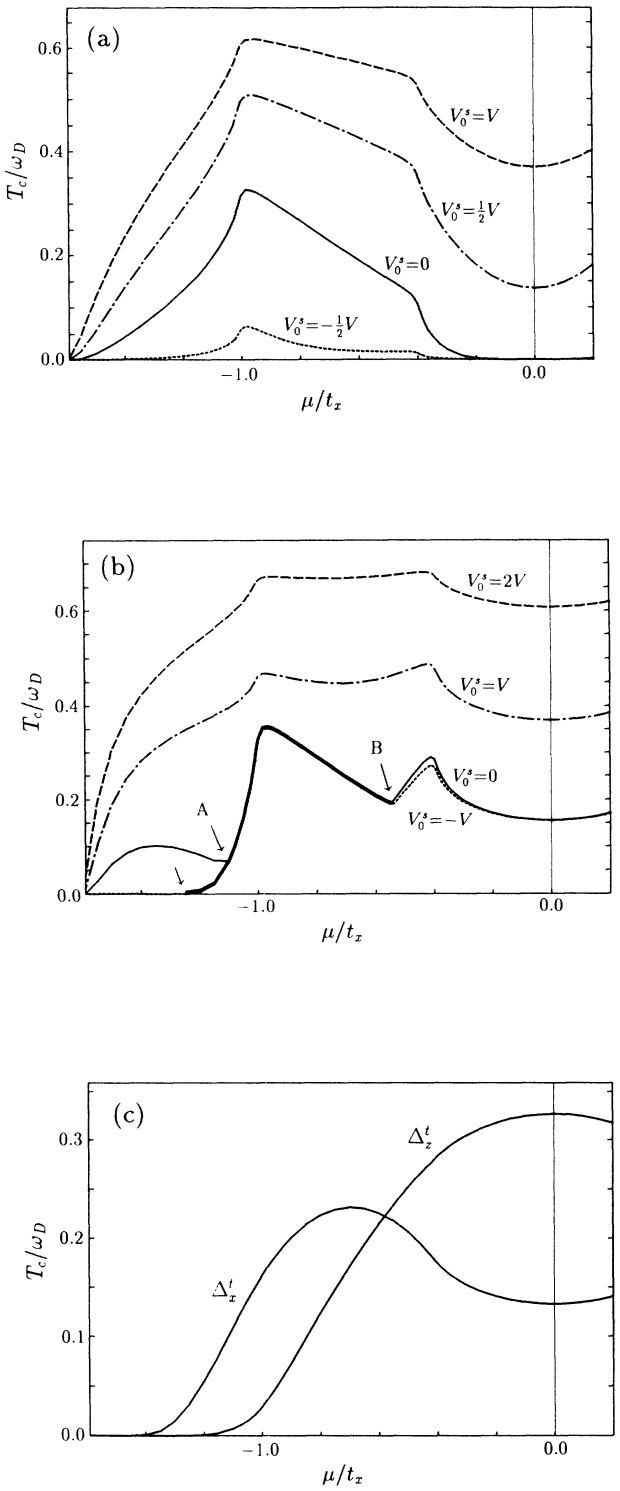

FIG. 3. T_c vs μ for the quasi-one-dimensional material ($\frac{3}{10}t_z=t_x=t_y$). (a) The case of singlet pairing in the presence of the on-site and intrachain intersite interaction, $V_z^s=V$, $V_x^s=V_y^s=0$. (b) The case of singlet pairing in the presence of the intrachain (on site) and interchain interaction, $V_x^s=V_y^s=V$, $V_z^s=0$. The bold line represents the d-symmetry region. (c) The case of triplet pairing in the quasi-one-dimensional system. The curve marked Δ_z^t represents the case $V_z^t=V$, $V_x^t=V_y^t=0$, and Δ_x^t represents the case $V_z^t=0$, $V_x^t=V_y^t=V$.

from Eqs. (22) and (24). The off-diagonal elements vanish because of the symmetry; the negative sign should be chosen in the parentheses of Eq. (22) for the triplet state, but the switching between the state of $\Delta_x^t \neq 0$ and that of $\Delta_z^t \neq 0$ may occur by changing μ.

C. Cubic material

Next, we discuss the transition temperature of the cubic system ($t_x = t_y = t_z$, $V_x^v = V_y^v = V_z^v$). $\lambda_{\max}$ is the largest one of

$$\lambda_s^s = \tfrac{1}{2}((2N_{xy}^s + N_{xx}^s)V_x^s + N_{00}^s V_0^s + \{[(2N_{xy}^s + N_{xx}^s)V_x^s - N_{00}^s V_0^s]^2 + 12N_{0x}^{s2} V_0^s V_x^s\}^{1/2}) , \tag{31}$$

$$\lambda_d^s = (N_{xx}^s - N_{xy}^s)V_x^s , \tag{32}$$

$$\lambda^t = N_{xx}^t V_x^t . \tag{33}$$

Figure 2(a) shows the μ dependence of T_c for the singlet pairing in the presence of the on-site and intersite interactions. We set $V_x^s = V_y^s = V_z^s = V$ in all lines. As in the case of Fig. 1(c), the s-symmetry state is realized to the left of the arrow, while the d-symmetry state appears to the right of the arrow (thick line). Again it can be seen that the repulsive on-site interaction suppresses the s-wave pairing, while the d-wave pairing is not affected.

Figure 2(b) shows μ dependence of T_c for the triplet pairing in the cubic system. The curve is smooth and there is no sharp structure reflecting the DOS.

D. Quasi-one-dimensional material

For the quasi-one-dimensional materials, the formalisms are the same as those of the layered materials. The ratio of the transfer integrals is only different, i.e., $t_z > t_x = t_y$. However, the μ dependence of T_c is quite different from the layered material as will be seen later. This is understood by the fact that the Fermi surface of the quasi-one-dimensional system has a planar shape, while that of the layered system has a cylindrical shape. In the following calculations, we set $t_x = t_y = \frac{3}{10} t_z$.

Figure 3(a) shows the μ dependence of T_c for the singlet pairing for the case of the finite on-site interaction and intrachain intersite interaction in the absence of the interchain interactions. $V_z^s = V$, $V_x^s = V_y^s = 0$ is assumed in all curves. $\lambda_{\max}$ is determined by Eq. (26) for this case. When the on-site interaction is reduced and becomes repulsive, T_c is diminished in the whole region of μ. This is a different feature from the case of the interlayer pairing [Fig. 1(a)] in which repulsive V_0^s does not reduce T_c. This is caused by the large mixing between the on-site pairing (Δ_0^s) and the intrachain intersite pairing (Δ_z^s). The quantity N_{0z}^s for the quasi-one-dimensional material is much larger than the corresponding quantity for the layered material.

Figure 3(b) shows the case of the intrachain on-site and interchain interactions for the singlet pairing. $V_x^s = V_y^s = V$, $V_z^s = 0$ is assumed in all curves. If the on-site attractive interaction V_0^s is strong, only the s-symmetry state is realized for all the μ region ($V_0^s = 2V, V$). With the decrease of the onsite interaction, the switching of the symmetry between the s and d states occurs twice. For example, for the case of the solid line ($V_0^s = 0$), the switching occurs at the point A and B. The d-symmetry state appears between A and B (thick line), and the s-symmetry states occurs in the outer sides of A and B. An interesting point is that not only for the d-wave pairing, but also for the s-wave pairing on the right-hand side of the point B, T_c is hardly affected by the repulsive V_0^s. On the other hand, the s-wave pairing on the left-hand side of the point A is reduced by the repulsive V_0^s. This property can be explained by the smallness of the ratio of Δ_0^s on the right-hand side of B.

Figure 3(c) shows the dependence of T_c on μ for the case of the triplet pairing. The curve marked Δ_z^t represents T_c for the case of $V_z^t = V$, $V_x^t = V_y^t = 0$, while Δ_x^t shows T_c for the case of $V_z^t = 0$, $V_x^t = V_y^t = V$. The curve of T_c versus μ marked Δ_z^t shows only a broad peak at the band center, while the peak of the curve marked Δ_x^t is shifted to the region of the higher DOS. [The DOS is not shown here, but it looks qualitatively like the dashed line ($V_0^s = V$) in Fig. 3(a).] This difference is caused by the characteristics of N_{zz}^t or N_{xx}^t, i.e., DOS weighted by the form factor of the pair. Namely, for the case of N_{zz}^t, the form factor is $\sin^2(k_z S_z)$, while that for N_{xx}^t is $\sin^2(k_x S_x)$ [see Eq. (22)]. In the former case, the μ dependence of the DOS is much changed by the form factor. This is why the curve of T_c versus μ marked Δ_z^t shows a quite different shape as compared to the DOS of the energy band, while the curve marked by Δ_x^t reflects DOS.

IV. MULTICOMPONENT GL EQUATION

To discuss the macroscopic properties of the superconductor in the presence of the magnetic field, we derive a multicomponent GL equation. It takes account not only of the center-of-mass coordinate, but also of the relative coordinate dependence of the order parameter by means of the multicomponents of the order parameter.

From Eqs. (10) and (11), we can derive a gap equation in terms of the normal-state Green's functions in the presence of the magnetic field, G_σ^0, as

$$\begin{aligned}\Delta_{\sigma\sigma'}^{*0}(\mathbf{j},\mathbf{j}+\boldsymbol{l})/V_l^0 &= -\Delta_{\sigma'\sigma}^{*1}(\mathbf{j},\mathbf{j}+\boldsymbol{l})/V_l^1 \\ &= \sum_{\omega_n}\sum_{\mathbf{j}_1}\sum_{\boldsymbol{l}_1}\sum_{i_1} G_\sigma^0(\mathbf{j}_1,\mathbf{j},-\omega_n)\Delta_{\sigma\sigma'}^{*i_1}(\mathbf{j}_1,\mathbf{j}_1+\boldsymbol{l}_1)G_{\sigma'}^0(\mathbf{j}_1+\boldsymbol{l}_1,\mathbf{j}+\boldsymbol{l},\omega_n) \\ &\quad + \sum_{\omega_n}\sum_{\mathbf{j}_1\mathbf{j}_2\mathbf{j}_3}\sum_{\boldsymbol{l}_1\boldsymbol{l}_2\boldsymbol{l}_3}\sum_{i_1 i_2 i_3}\sum_{\sigma_1} G_\sigma^0(\mathbf{j}_1,\mathbf{j},-\omega_n)\Delta_{\sigma\sigma'}^{*i_1}(\mathbf{j}_1,\mathbf{j}_1+\boldsymbol{l}_1)G_{\sigma'}^0(\mathbf{j}_1+\boldsymbol{l}_1,\mathbf{j}_2,\omega_n)\Delta_{\sigma'\sigma_1}^{i_2}(\mathbf{j}_2,\mathbf{j}_2+\boldsymbol{l}_2) \\ &\quad \times G_{\sigma_1}^0(\mathbf{j}_3,\mathbf{j}_2+\boldsymbol{l}_2,-\omega_n)\Delta_{\sigma_1\sigma'}^{*i_3}(\mathbf{j}_3,\mathbf{j}_3+\boldsymbol{l}_3)G_{\sigma'}^0(\mathbf{j}_3+\boldsymbol{l}_3,\mathbf{j}+\boldsymbol{l},\omega_n) .\end{aligned} \tag{34}$$

After some straightforward calculations, we obtain the first-order terms of Eq. (34) in the notation of Δ_{ℓ}^{ν} defined in Eqs. (13)–(16) as

$$\Delta_{\ell}^{\nu*(1)}/V_{\ell}^{\nu} \equiv \sum_{\ell'} \sum_{X,Y=x,y,z} \left[{}^{\nu}K_{\ell\ell'} + {}^{\nu}P_{\ell\ell'}^{X} \frac{\partial}{\partial X} + {}^{\nu}P_{\ell\ell'}^{XY} \frac{\partial^2}{\partial X \partial Y} + {}^{\nu}K_{\ell\ell'}^{XY} \left[2ieA_X + \frac{\partial}{\partial X} \right] \left[2ieA_Y + \frac{\partial}{\partial Y} \right] \right] \Delta_{\ell'}^{\nu*} , \tag{35}$$

where, $\nu = s,t$ and the coefficients, K's and P's, are defined as

$${}^{\nu}K_{\ell\ell'} = \frac{S_x S_y S_z T}{2(2\pi)^3} \sum_{\omega_n} \int d\mathbf{k} \frac{(e^{i\mathbf{k}\cdot\boldsymbol{l}} \pm e^{-i\mathbf{k}\cdot\boldsymbol{l}})(e^{-i\mathbf{k}\cdot\boldsymbol{l}'} \pm e^{i\mathbf{k}\cdot\boldsymbol{l}'})}{\omega_n^2 + \varepsilon_{\mathbf{k}}^2} , \tag{19}$$

$${}^{\nu}P_{\ell\ell'}^{X} = -\frac{S_x S_y S_z T}{4(2\pi)^3} \sum_{\omega_n} \int d\mathbf{k} (e^{i\mathbf{k}\cdot\boldsymbol{l}} \pm e^{-i\mathbf{k}\cdot\boldsymbol{l}})(e^{-i\mathbf{k}\cdot\boldsymbol{l}'} \pm e^{i\mathbf{k}\cdot\boldsymbol{l}'}) \frac{(\delta_{\ell' X} - \delta_{\ell X})}{\omega_n^2 + \varepsilon_{\mathbf{k}}^2} , \tag{36}$$

$${}^{\nu}P_{\ell\ell'}^{XY} = \frac{S_x S_y S_z T}{8(2\pi)^3} \sum_{\omega_n} \int d\mathbf{k} (e^{i\mathbf{k}\cdot\boldsymbol{l}} \pm e^{-i\mathbf{k}\cdot\boldsymbol{l}})(e^{-i\mathbf{k}\cdot\boldsymbol{l}'} \pm e^{i\mathbf{k}\cdot\boldsymbol{l}'}) \frac{(\delta_{\ell' X} - \delta_{\ell X})(\delta_{\ell' Y} - \delta_{\ell Y})}{\omega_n^2 + \varepsilon_{\mathbf{k}}^2} , \tag{37}$$

$$\begin{aligned} {}^{\nu}K_{\ell\ell'}^{XY} = -\frac{S_x S_y S_z T}{8(2\pi)^3} \sum_{\omega_n} \int d\mathbf{k} (e^{i\mathbf{k}\cdot\boldsymbol{l}} \pm e^{-i\mathbf{k}\cdot\boldsymbol{l}})(e^{-i\mathbf{k}\cdot\boldsymbol{l}'} \pm e^{i\mathbf{k}\cdot\boldsymbol{l}'}) \\ \times \left[\frac{2S_X t_X \sin(k_X S_X) S_Y t_Y \sin(k_Y S_Y)}{(\omega_n^2 + \varepsilon_{\mathbf{k}}^2)^2} \left[1 - \frac{4\omega_n^2}{\omega_n^2 + \varepsilon_{\mathbf{k}}^2} \right] - \frac{2\varepsilon_{\mathbf{k}} S_X^2 t_X \cos(k_X S_X)}{(\omega_n^2 + \varepsilon_{\mathbf{k}}^2)^2} \delta_{XY} \right] , \end{aligned} \tag{38}$$

where $+$ is for $\nu = s$ and $-$ is for $\nu = t$. At first glance, the second and the third terms in the large square brackets of the right-hand side of Eq. (35) seem to break the gauge invariance, but actually this is not so. This is easily verified by taking account of the phase relation between the order parameters with different $\boldsymbol{l}$.

After some straightforward calculations, we obtain the third-order terms of Eq. (34) in the notation of Δ_{ℓ}^{s}, Δ_{ℓ}^{0}, and $\Delta_{\ell}^{\pm 1}$ defined by Eqs. (13)–(17) as

$$\Delta_{\ell}^{s*(3)} \equiv -2E_{\ell s \ell_1 s \ell_2 s \ell_3} \Delta_{\ell_1}^{s*} \Delta_{\ell_2}^{s} \Delta_{\ell_3}^{s*} + E_{\ell s \ell_1 t \ell_2 t \ell_3} \Delta_{\ell_1}^{s*} (2\Delta_{\ell_2}^{0} \Delta_{\ell_3}^{0*} + \Delta_{\ell_2}^{+1} \Delta_{\ell_3}^{+1*} + \Delta_{\ell_2}^{-1} \Delta_{\ell_3}^{-1*}) , \tag{39}$$

$$\Delta_{\ell}^{0*(3)} \equiv -2E_{\ell t \ell_1 s \ell_2 s \ell_3} \Delta_{\ell_1}^{0*} \Delta_{\ell_2}^{s} \Delta_{\ell_3}^{s*} + E_{\ell t \ell_1 t \ell_2 t \ell_3} \Delta_{\ell_1}^{0*} (2\Delta_{\ell_2}^{0} \Delta_{\ell_3}^{0*} + \Delta_{\ell_2}^{+1} \Delta_{\ell_3}^{+1*} + \Delta_{\ell_2}^{-1} \Delta_{\ell_3}^{-1*}) , \tag{40}$$

$$\Delta_{\ell}^{\pm 1*(3)} \equiv -2E_{\ell t \ell_1 s \ell_2 s \ell_3} \Delta_{\ell_1}^{\pm 1*} \Delta_{\ell_2}^{s} \Delta_{\ell_3}^{s*} + 2E_{\ell t \ell_1 t \ell_2 t \ell_3} \Delta_{\ell_1}^{\pm 1*} (\Delta_{\ell_2}^{0} \Delta_{\ell_3}^{0*} + \Delta_{\ell_2}^{\pm 1} \Delta_{\ell_3}^{\pm 1*}) , \tag{41}$$

where

$$E_{\ell \nu_1 \ell_1 \nu_2 \ell_2 \nu_3 \ell_3} = \frac{S_x S_y S_z T}{(2\pi)^3} \sum_{\omega_n} \int d\mathbf{k} \frac{e^{i\mathbf{k}\cdot\boldsymbol{l}}}{(\omega_n^2 + \varepsilon_{\mathbf{k}}^2)^2} \begin{Bmatrix} \cos(\mathbf{k}\cdot\boldsymbol{l}_1) \\ -i \sin(\mathbf{k}\cdot\boldsymbol{l}_1) \end{Bmatrix} \begin{Bmatrix} \cos(\mathbf{k}\cdot\boldsymbol{l}_2) \\ -i \sin(\mathbf{k}\cdot\boldsymbol{l}_2) \end{Bmatrix} \begin{Bmatrix} \cos(\mathbf{k}\cdot\boldsymbol{l}_3) \\ -i \sin(\mathbf{k}\cdot\boldsymbol{l}_3) \end{Bmatrix} . \tag{42}$$

In the preceding curly braces, $\cos(\mathbf{k}\cdot\boldsymbol{l}_n)$ should be chosen for $\nu_n = s$, and $-i \sin(\mathbf{k}\cdot\boldsymbol{l}_n)$ should be chosen for $\nu_n = t$.

An interesting point about the third-order terms is the existence of the mixing terms between the different symmetry states. Even for the mixing between the spin singlet and triplet states, the coefficient E is not zero. This fact indicates the possibility of the coexistence of the two types of the pairing states below the transition temperature.[11,12]

V. UPPER-CRITICAL FIELD H_{c2}

One can obtain the upper-critical field H_{c2} near T_c from Eq. (35). We choose the vector potential as $\mathbf{A} = (0, xH \sin\theta, -xH \cos\theta)$ so that the magnetic field becomes $\mathbf{H} = (0, H\cos\theta, H\sin\theta)$. For the spin singlet pair, we obtain

$$\left[{}^{s}K_{\ell\ell'} - \frac{1}{V_{\ell}^{s}} + {}^{s}P_{\ell\ell'}^{x} \frac{d}{dx} + {}^{s}\tilde{K}_{\ell\ell'}^{xx} \frac{d^2}{dx^2} - 4e^2H^2x^2({}^{s}K_{\ell\ell'}^{yy} \sin^2\theta + {}^{s}K_{\ell\ell'}^{zz} \cos^2\theta) \right] \Delta_{\ell'}^{s*} = 0 , \tag{43}$$

where ${}^{s}\tilde{K}_{\ell\ell'}^{xx} = {}^{s}K_{\ell\ell'}^{xx} + {}^{s}P_{\ell\ell'}^{xx}$. For the spin triplet pair, the equation for H_{c2} is written as

$$\left[{}^{t}K_{\ell\ell'} - \frac{1}{V_{\ell}^{t}} + {}^{t}K_{\ell\ell'}^{xx} \frac{d^2}{dx^2} - 4e^2H^2x^2({}^{t}K_{\ell\ell'}^{yy} \sin^2\theta + {}^{t}K_{\ell\ell'}^{zz} \cos^2\theta) + 2ieH({}^{t}K_{xy}^{xy} \sin\theta - {}^{t}K_{xz}^{xz} \cos\theta) \left[2x \frac{d}{dx} + 1 \right] \right] \Delta_{\ell'}^{t*} = 0 . \tag{44}$$

${}^tP_{\ell\ell'}$'s are zero for the spin triplet pair, while ${}^sK^{XY}_{\ell\ell'}$'s ($X\neq Y$) are zero for the spin singlet pair.

To solve Δ^ν_ℓ from the Eqs. (43) or (44), we have performed a variational calculation by taking the trial functions of $\Delta_\ell(x)$ as

$$\Delta_\ell(x)=\exp\left[-\frac{\gamma_\ell eH}{2}x^2\right]\sum_n C_{\ell n}H_n(x)\ , \tag{45}$$

where $H_n(x)$ is the Hermite polynomial. We have taken account of $n=0$–4, but we found that the obtained result is not so much changed with the number of the included terms of Eq. (45), and the result was also unchanged by taking different values of γ_ℓ for different ℓ. Therefore, in the following we discuss H_{c2}, assuming the form of $\Delta_\ell(x)$ as

$$\Delta_\ell(x)=\Delta_\ell\exp\left[-\frac{\gamma eH}{2}x^2\right]\ . \tag{46}$$

For a rigorous quantitative discussion, the expansion coefficients C_{ln} should be determined carefully particularly in the case of the p-wave pairing. This can be worked out, for example, by finding a recursion relation for the coefficients as performed by Scharnberg and Klemm.[13,14] We expect, however, the preceding approximation is valid for our qualitative discussions. Then, Eqs. (43) and (44) are reduced to

$$\sum_{\ell'}\left[{}^\nu K_{\ell\ell'}-\frac{\delta_{\ell\ell'}}{V^\nu_\ell}\right]\Delta^\nu_{\ell'} =\frac{H}{2}\sum_{\ell'}[{}^\nu\tilde{K}^{xx}_{\ell\ell'}\gamma+4({}^\nu K^{yy}_{\ell\ell'}\sin^2\theta +{}^\nu K^{zz}_{\ell\ell'}\cos^2\theta)/\gamma]\Delta^\nu_{\ell'}\ . \tag{47}$$

The upper-critical field H_{c2} is obtained by the maximum of the largest eigenvalue of the preceding secular equation as the function of γ.

A. Nondegenerate system

Figure 4 shows the angle dependence of H_{c2} for the case of the interlayer pairing for the layered system corresponding to Figs. 1(a) and 1(b). The solid line marked Δ^s_z corresponds to the singlet pairing ($V^s_z\neq 0$, $V^s_0=V^s_x=V^s_y=0$), and the dashed line marked Δ^t_z corresponds to the triplet pairing ($V^t_z\neq 0$, $V^t_x=V^t_y=0$). The case of the on-site pairing ($V^s_0\neq 0$, $V^s_x=V^s_y=V^s_z=0$) is also shown as the dotted line (Δ^s_0). This is the clearest case to demonstrate how the existence of the anisotropic pairing (intersite pairing) affects the macroscopic anisotropy. The anisotropy $H_{c2}(0)/H_{c2}(\pi/2)$ is determined by the ratio ${}^\nu K^{yy}_{\ell\ell'}/{}^\nu K^{zz}_{\ell\ell'}$ as follows. For the case with single nonzero component Δ^ν_ℓ of the pair potential, $H_{c2}(\theta)$ is given by

$$H_{c2}(\theta)\propto\frac{{}^\nu K_{\ell\ell}-1/V^\nu_\ell}{[{}^\nu\tilde{K}^{xx}_{\ell\ell}({}^\nu K^{yy}_{\ell\ell}\sin^2\theta+{}^\nu K^{zz}_{\ell\ell}\cos^2\theta)]^{1/2}}\ . \tag{48}$$

Therefore it holds

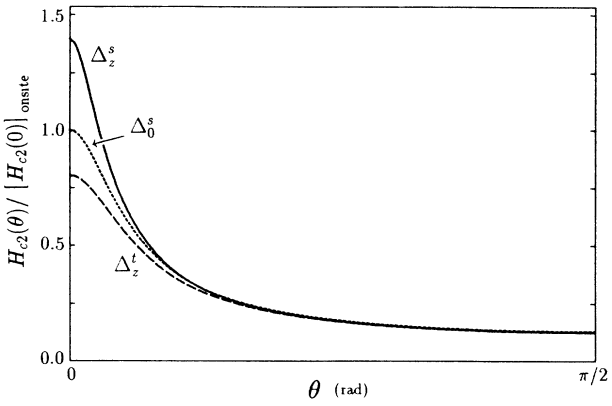

FIG. 4. H_{c2} vs θ for Δ^s_z, singlet interlayer pairing ($V^s_z\neq 0$, $V^s_0=V^s_x=V^s_y=0$); Δ^t_z, triplet interlayer pairing ($V^t_z\neq 0$, $V^t_x=V^t_y=0$); and Δ^s_0, singlet intralayer (on site) pairing ($V^s_0\neq 0$, $V^s_x=V^s_y=V^s_z=0$). Here $t_x=t_y=10t_z$ and $S_x=S_y=S_z$. θ represents the angle between the applied field and the xy plane.

$$\frac{H_{c2}(0)}{H_{c2}(\pi/2)}=\left[\frac{{}^\nu K^{yy}_{\ell\ell}}{{}^\nu K^{zz}_{\ell\ell}}\right]^{1/2}\ . \tag{49}$$

The effect of the intersite pairing on the anisotropy of H_{c2} can be seen by the ratio

$$\left[\frac{H_{c2}(0)}{H_{c2}(\pi/2)}\right]_{\text{intersite}}\left[\frac{H_{c2}(\pi/2)}{H_{c2}(0)}\right]_{\text{on site}} =({}^sK^{zz}_{00}{}^\nu K^{yy}_{\ell\ell}/{}^sK^{yy}_{00}{}^\nu K^{zz}_{\ell\ell})^{1/2}\ . \tag{50}$$

For the case of the cylindrical Fermi surface, one can confirm that

$$\frac{{}^sK^{zz}_{00}}{{}^sK^{yy}_{00}}\frac{{}^sK^{yy}_{zz}}{{}^sK^{zz}_{zz}}\approx 2\ , \tag{51}$$

$$\frac{{}^sK^{zz}_{00}}{{}^sK^{yy}_{00}}\frac{{}^tK^{yy}_{zz}}{{}^tK^{zz}_{zz}}\approx\frac{2}{3}\ . \tag{52}$$

Using the preceding ratios for Eq. (50), we can explain the relative values of $H_{c2}(0)$ of the three cases in Fig. 4.

When $\lambda_{\max}$, which determines T_c is not degenerate, the angle dependence of H_{c2} is given by Eq. (48), which is the same as the one given by the effective mass approximation:[15]

$$H_{c2}(\theta)=\frac{H_0}{(a\cos^2\theta+b\sin^2\theta)^{1/2}}\ . \tag{53}$$

Thus, in this paper, we obtain the microscopic expressions of the parameters a and b by the multicomponent GL equation:

$$a\propto{}^\nu K^{zz}_{\ell\ell},\ b\propto{}^\nu K^{yy}_{\ell\ell}\ . \tag{54}$$

In Fig. 5, we show the V^s_z/V^s_0 or V^s_x/V^s_0 dependence of the anisotropy ratio, $H_{c2}(0)/H_{c2}(\pi/2)=\sqrt{b/a}$, in the layered system. We varied the parameter as

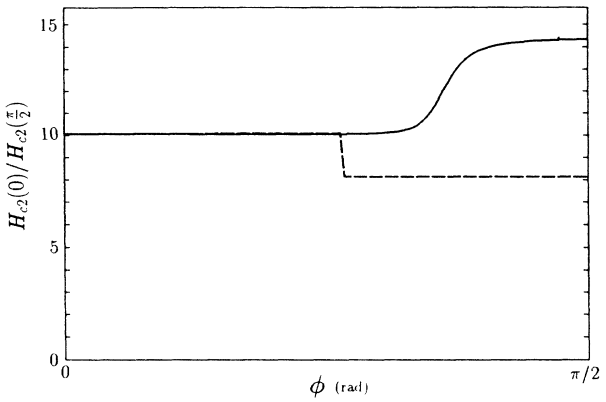

FIG. 5. $H_{c2}(0)/H_{c2}(\pi/2)$ vs ϕ in the layered system. The relative magnitudes of the interactions are changed with ϕ as $[V_0^s = V\cos\phi,\ V_z^s = V\sin\phi,\ V_x^s = V_y^s = 0]$ for the solid line, and $[V_0^s = V\cos\phi,\ V_x^s = V_y^s = V\sin\phi,\ V_z^s = 0]$ for the dashed line.

$$\begin{aligned} &V_0^s = V\cos^2\phi,\ V_z^s = V\sin^2\phi, \quad \text{for the solid line} \\ &V_0^s = V\cos^2\phi,\ V_x^s = V\sin^2\phi, \quad \text{for the dashed line} . \end{aligned} \tag{55}$$

The solid line (on-site and interlayer pairing) shows that the anisotropy ratio switches at certain values of V_z^s/V_0^s rather smoothly. This rounding effect, which comes from the mixing of Δ_0^s and Δ_z^s, was analyzed in our previous paper. On the other hand, the dashed line (on-site and intralayer intersite pairing) shows that the anisotropy ratio changes its value sharply. This behavior is consistent with the sharp switching of the order parameter from the s pairing to the d pairing in Fig. 1(c).

Figure 6 shows the μ dependence of

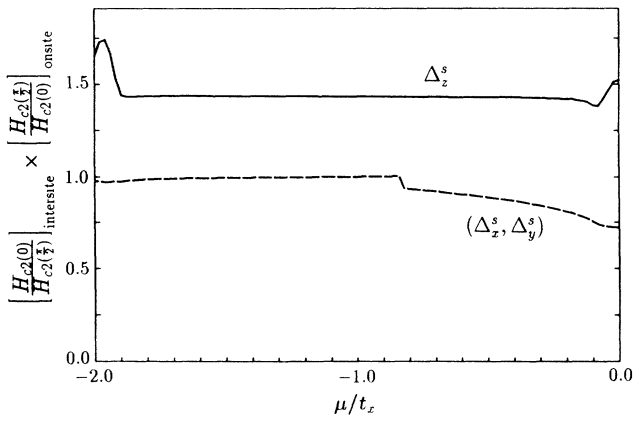

FIG. 6. μ dependence of

$$[H_{c2}(0)/H_{c2}(\pi/2)]_{\text{intersite}}/[H_{c2}(0)/H_{c2}(\pi/2)]_{\text{on site}} .$$

The solid line marked Δ_z^s shows the case of the interlayer pairing ($V_z^s \neq 0$, $V_0^s = V_x^s = V_y^s = 0$), and the dashed line marked (Δ_x^s, Δ_y^s) shows the case of the intralayer intersite pairing ($V_x^s = V_y^s \neq 0$, $V_0^s = V_z^s = 0$).

$$\left[\frac{H_{c2}(0)}{H_{c2}(\pi/2)}\right]_{\text{intersite}} \Big/ \left[\frac{H_{c2}(0)}{H_{c2}(\pi/2)}\right]_{\text{on site}}$$

for the layered system. The solid line marked Δ_z^s corresponds to the case of $V_z^s \neq 0$, $V_x^s = V_y^s = V_0^s = 0$. It is found that the singlet interlayer pairing always enhances the anisotropy by the factor of 1.4 compared to that of the on-site pairing as far as the system has a cylindrical Fermi surface. On the other hand, the dashed line marked (Δ_x^s, Δ_y^s) corresponding to the case $V_x^s = V_y^s \neq 0$, $V_0^s = V_z^s = 0$ shows that the d-wave pairing by the intralayer intersite interaction reduces its anisotropy. The value of the reduction ratio (dashed line) depends on μ, while the enhanced ratio of the interlayer pairing case (solid line) is hardly dependent on μ. The dashed line takes the value of 1 at the left side of the point $\mu \approx -0.85 t_x$, where the d-wave state changes to the s-wave state. It is an interesting point that though the dashed line assumes the intersite interaction alone ($V_0^s = 0$), the anisotropy ratio in the s-wave region is equal to 1. This suggests an answer to the question raised in Sec. I. Namely, it is clarified here that if the order parameter has s symmetry, the presence of the intersite interaction does not affect the anisotropy of the macroscopic property such as H_{c2}, while d- or p-symmetry states affect its macroscopic anisotropy.

B. Degenerate system

For the system where $\lambda_{\max}$ is degenerate, we obtained the result that the angle dependence of H_{c2} can show an anomalous behavior that cannot be fitted by the effective mass model [Eq. (53)]. Some examples of the degenerate system are described in the following.

Figure 7(a) shows the angle dependence of H_{c2} for the case of the degenerate state of the interlayer pairing and the intralayer intersite d pairing. The solid line shows the angle dependence of H_{c2} calculated by Eq. (47) and the dashed curve is the line fitted by Eq. (53). The three lines plotted at the bottom represent the three components Δ_x^s, Δ_y^s, and Δ_z^s of the eigenvector. It can be seen from this plot that the interlayer pairing (Δ_z^s) dominates in the smaller θ region and the intralayer intersite pairing (Δ_x^s, Δ_y^s) dominates in the larger θ region. This change occurs because two states are equally possible to realize (i.e., the system is degenerate) and the applied field favors either type of the pairing according to its direction. This means that a phase transition is induced by the rotation of the magnetic field.

Figure 7(b) shows the case of the triplet pairing. Here Δ_x^t, Δ_y^t, and Δ_z^t are all degenerate. However, only the state with nonzero Δ_y^t (smaller θ region) and the state with nonzero Δ_z^t (larger θ region) are realized. The preferred axis of the triplet pair is parallel to the magnetic field, e.g., when $\mathbf{H} = \mathbf{e}_z$, the state with Δ_z^t is the most stable. On the other hand, the preferred axis of the singlet pair is perpendicular to $\mathbf{H}$. This originates from the fact that the singlet intersite pair perpendicular to $\mathbf{H}$ enhances H_{c2}, while the triplet pair perpendicular to $\mathbf{H}$ reduces H_{c2} (Fig. 4). The switching of the symmetry in

Fig. 7(b) is sharp as compared with the Fig. 7(a). This is again due to the diagonal form of the ${}^tK_{\ell\ell'}$ matrices for the triplet pairing case.

The preceding two examples, Figs. 7(a) and 7(b), are the cases of rather accidental degeneracy, since the allowable region of the parameter (the ratio, V_x/V_z) is very narrow. These types of accidental degeneracy are possible in many ways, for example, the p-wave state and the d-wave state, the d-wave state and the s-wave state, etc. Though the parameter region is narrow, if there is a material that changes the symmetry of its order parameter by controlling other parameters (such as chemical potential), it is possible to set the material to degenerate.

On the other hand, some materials can be degenerate

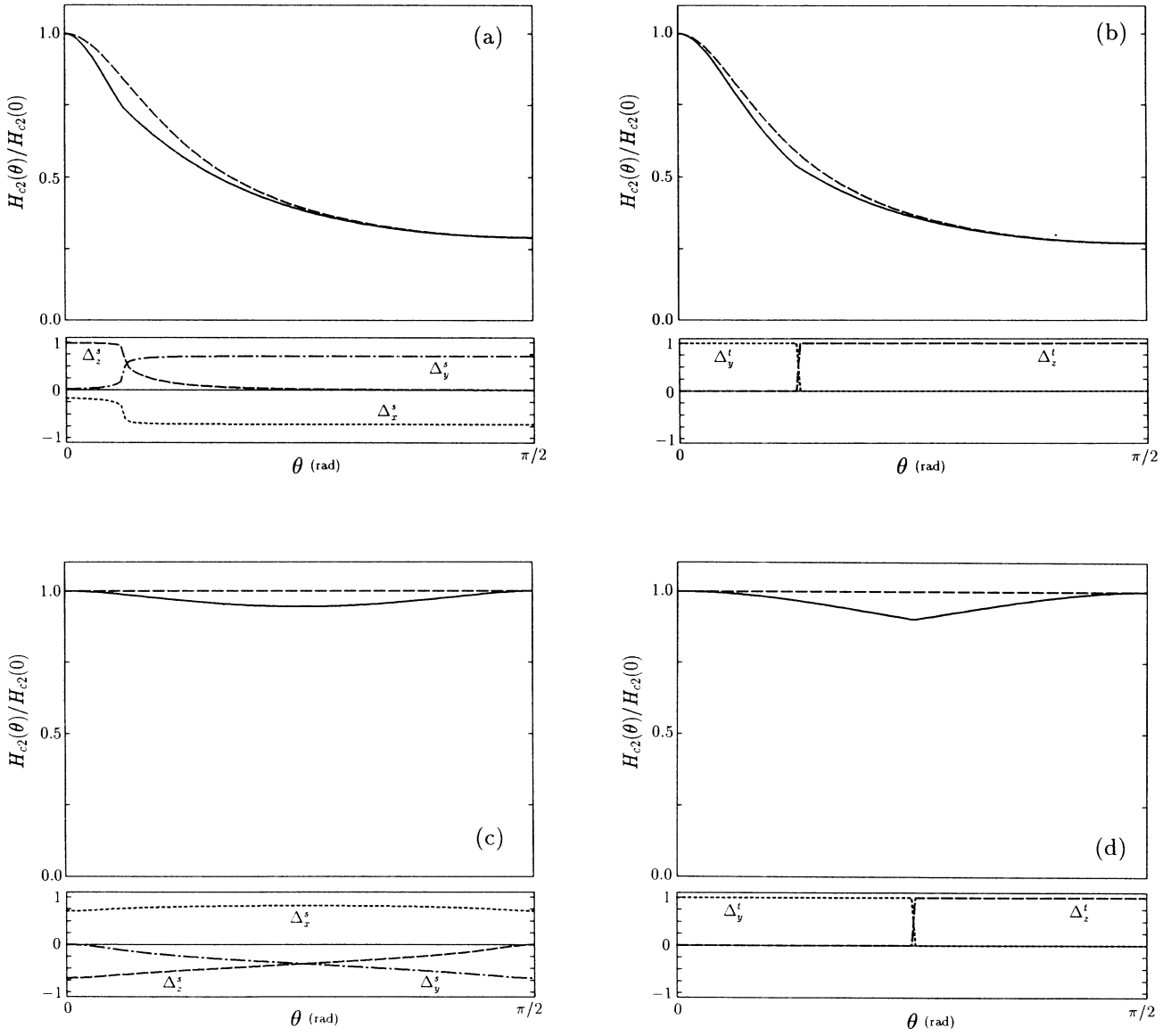

FIG. 7. The angle dependence of H_{c2}. θ represents the direction of the applied field in the yz plane. When the field is parallel to the y axis, $\theta=0$. The relative phase of the order parameter is shown together. (a) The case of accidental degeneracy of the singlet interlayer and intralayer intersite d pairing. The switching of the relative phase of the order parameter can be seen. (b) The case of accidental degeneracy of the triplet interlayer and intralayer intersite pairing, i.e., Δ_x^t, Δ_y^t, and Δ_z^t are all degenerate. (c) The case of singlet intersite (d-wave) pairing in the cubic system. A gradual change of the relative phase can be seen. (d) The case of triplet intersite pairing in the cubic system. There is a cusp point at the center of the figure reflecting the sharpness of the phase switching.

naturally. The natural degeneracies available in our model are singlet: $(\Delta_x^s,\Delta_y^s,\Delta_z^s)=(1,-1,0)$ and $(0,1,-1)$ in the cubic system, triplet: $(\Delta_x^t,\Delta_y^t,\Delta_z^t)=(1,0,0)$ and $(0,1,0)$ in the tetragonal system, and triplet: $(\Delta_x^t,\Delta_y^t,\Delta_z^t)=(1,0,0)$, $(0,1,0)$ and $(0,0,1)$ in the cubic system.

Figure 7(c) shows the angle dependence of H_{c2} for the case of the singlet pairing in the cubic material. It can be seen that when $\mathbf{H}=(0,H,0)$, then $\Delta=(1,0,-1)$ and when $\mathbf{H}=(0,0,H)$, then $\Delta=(1,-1,0)$. The point of the switching cannot be defined in this case since the eigenvector changes gradually when the magnetic field is rotated.

Figure 7(d) shows H_{c2} for the case of the triplet pairing in the cubic system. It is possible to think of this figure as the angle dependence of H_{c2} in the basal plane of the tetragonal system for the triplet pairing. When $\mathbf{H}=(0,H,0)$, then $\Delta=(0,1,0)$ and when $\mathbf{H}=(0,0,H)$, then $\Delta=(0,0,1)$. There is a cusp at the center of the figure reflecting the sharpness of the switching of the order parameter.

These types of H_{c2} anisotropy, due to degeneracy, are studied theoretically by several authors.[16–18] However, in their analysis, they did not appropriately estimate the off-diagonal coefficients in the GL equation, which is essential in this H_{c2} anisotropy, and therefore their analyses are rather phenomenological. We estimated the coefficients from microscopic theory so that our estimation of the ratio, $H_{c2}(0)/H_{c2}(\pi/4)$, is more realistic. Furthermore, our result shows that, in the case of the triplet pairing, there is a sharp cusp point at $\theta=\pi/4$, which was not predicted previously.

VI. CONCLUSION AND DISCUSSION

We investigated the superconductivity in the tight-binding picture taking account of the intersite pairing as well as the on-site pairing. First, for the uniform system, we derived a linearized equation of the order parameters, each component of which represents the different intersite pairing. Based on that equation, the transition temperature and the symmetry of the pair wave function (Tables I–III) were discussed. For the layered material, the transition temperature T_c for the p- and d-symmetry state decreases sharply when the chemical potential is moved from the band center, while T_c for the s-symmetry state decreases only gradually. This is the effect of the form factor, $\cos(k_l S_l)$ or $\sin(k_l S_l)$ representing the intersite pair. This feature cannot be described by the continuum model. It should be remarked that the p- or d-

TABLE I. Classification for the singlet pairing in the layered material and the quasi-one-dimensional material investigated in this paper. The values of a and b depend on the energy dispersion (t_x,t_y,t_z) and the coupling constants $(V_0^s,V_x^s,V_y^s,V_z^s)$.

	$V_z^s\neq0,\ V_0^s\neq0,\ V_x^s=V_y^s=0$	$V_z^s=0,\ V_0^s\neq0,\ V_x^s=V_y^s\neq0$
$t_z<t_x=t_y$ layered material	Pairing: Δ_0^s (intralayer), Δ_z^s (interlayer). State: $\begin{bmatrix}\Delta_0^s\\ \Delta_z^s\end{bmatrix}=\begin{bmatrix}a\\ b\end{bmatrix}$	Pairing: Δ_0^s (on site), Δ_x^s,Δ_y^s (intralayer intersite). State: $\begin{bmatrix}\Delta_0^s\\ \Delta_x^s\\ \Delta_y^s\end{bmatrix}=\begin{bmatrix}a\\ b\\ b\end{bmatrix}$ $\cdots$ s wave; $\begin{bmatrix}\Delta_0^s\\ \Delta_x^s\\ \Delta_y^s\end{bmatrix}=\begin{bmatrix}0\\ 1\\ -1\end{bmatrix}$ $\cdots$ d wave
$t_z>t_x=t_y$ quasi-one-dimensional material	Pairing: Δ_0^s (on site), Δ_z^s (intrachain intersite). State: $\begin{bmatrix}\Delta_0^s\\ \Delta_z^s\end{bmatrix}=\begin{bmatrix}a\\ b\end{bmatrix}$	Pairing: Δ_0^s (intrachain), Δ_x^s,Δ_y^s (interchain). State: $\begin{bmatrix}\Delta_0^s\\ \Delta_x^s\\ \Delta_y^s\end{bmatrix}=\begin{bmatrix}a\\ b\\ b\end{bmatrix}$ $\cdots$ s wave; $\begin{bmatrix}\Delta_0^s\\ \Delta_x^s\\ \Delta_y^s\end{bmatrix}=\begin{bmatrix}0\\ 1\\ -1\end{bmatrix}$ $\cdots$ d wave

TABLE II. Classification for the singlet pairing in the cubic material. There are two degenerate states for d symmetry, while there is only one state for s symmetry.

	$V_0^s \neq 0,\ V_x^s = V_y^s = V_z^s \neq 0$
$t_z = t_x = t_y$ cubic material	Pairing: Δ_0^s (on site); $\Delta_x^s, \Delta_y^s, \Delta_z^s$ (intersite)
	State: $\begin{pmatrix}\Delta_0^s\\ \Delta_x^s\\ \Delta_y^s\\ \Delta_z^s\end{pmatrix} = \begin{pmatrix}a\\ b\\ b\\ b\end{pmatrix}$ $\cdots$ s wave
	$\begin{pmatrix}\Delta_0^s\\ \Delta_x^s\\ \Delta_y^s\\ \Delta_z^s\end{pmatrix} = \begin{pmatrix}0\\ 1\\ -1\\ 0\end{pmatrix}, \begin{pmatrix}0\\ 0\\ 1\\ -1\end{pmatrix}$ $\cdots$ d wave

symmetry state at the band center in the layered system are favored compared to the s-symmetry state in the case of the repulsive on-site interaction. This fact would yield some suggestions to consider the mechanism of the high-T_c superconductivity.

In the latter half of this paper, we have derived a multicomponent GL equation that reflects the relative coordinate of the pair. The angle dependence of H_{c2} is discussed based on that equation. We obtained the result that, for the singlet pairing, the intersite pair perpendicular to the magnetic field enhances H_{c2}, while for the triplet pairing it reduces H_{c2}. For example, when $\mathbf{H} = H\mathbf{e}_x$, Δ_z^s enhances H_{c2}, while Δ_z^t reduces H_{c2}. This is explained by the fact that the motion of the pair in the perpendicular plane to the magnetic field is suppressed by the relative phase relation inside the pair for the singlet state, but enhanced for the triplet state.

We also obtained the result that the s-symmetry state shows the same anisotropy as the on-site pairing state, though the intersite interaction is strong. This suggests an answer to the question raised in Sec. I that if the order parameter has s symmetry, the presence of the intersite interaction does not affect the anisotropy of the macroscopic property such as H_{c2} while the d- or p-symmetry state affects its macroscopic anisotropy.

As far as the system is not degenerate, the angle dependence of H_{c2} is found to be given by the formula of the effective mass approximation. This means that in the nondegenerate case, the symmetry of the ordered state is not changed even when the direction of the magnetic field is changed, and a single type of ordered state leads to an angle dependence of the usual one-component GL model. However, if the two or more symmetry states are degenerate, the angle dependence of H_{c2} cannot be fitted by the simple effective mass approximation. In this case, the

TABLE III. Classification for the triplet pairing in the layered material, the quasi-one-dimensional material, and the cubic material. There are two degenerate states for the intralayer intersite pairing and the interchain pairing, respectively. The cubic material has three degenerate states.

	$V_z^t \neq 0,\ V_x^t = V_y^t \neq 0$
$t_z < t_x = t_y$ layered material	$\begin{pmatrix}\Delta_x^t\\ \Delta_y^t\\ \Delta_z^t\end{pmatrix} = \begin{pmatrix}0\\ 0\\ 1\end{pmatrix}$ $\cdots$ interlayer
	$\begin{pmatrix}\Delta_x^t\\ \Delta_y^t\\ \Delta_z^t\end{pmatrix} = \begin{pmatrix}1\\ 0\\ 0\end{pmatrix}, \begin{pmatrix}0\\ 1\\ 0\end{pmatrix}$ $\cdots$ intralayer intersite
$t_z > t_x = t_y$ quasi-one-dimensional material	$\begin{pmatrix}\Delta_x^t\\ \Delta_y^t\\ \Delta_z^t\end{pmatrix} = \begin{pmatrix}0\\ 0\\ 1\end{pmatrix}$ ..intrachain intersite
	$\begin{pmatrix}\Delta_x^t\\ \Delta_y^t\\ \Delta_z^t\end{pmatrix} = \begin{pmatrix}1\\ 0\\ 0\end{pmatrix}, \begin{pmatrix}0\\ 1\\ 0\end{pmatrix}$ $\cdots$ interchain
	$V_x^t = V_y^t = V_z^t \neq 0$
$t_z = t_x = t_y$ cubic material	$\begin{pmatrix}\Delta_x^t\\ \Delta_y^t\\ \Delta_z^t\end{pmatrix} = \begin{pmatrix}1\\ 0\\ 0\end{pmatrix}, \begin{pmatrix}0\\ 1\\ 0\end{pmatrix}, \begin{pmatrix}0\\ 0\\ 1\end{pmatrix}$ $\cdots$ intersite

switching between the different symmetry states occurs with the rotation of the magnetic field. This degeneracy probably occurs for the d-wave pairing in the cubic material and for the p-wave pairing in the tetragonal material. We expect the possibility that the measurement of the angle dependence of H_{c2} for UBe_{13}, cubic heavy-fermion superconductor, might reveal this anomalous angle dependence, if the pairing of this material is of the non-s-wave type. When the angle dependence is observed, one will be able to distinguish the pairing symmetry, p wave or d wave, from the shape of the $H_{c2}(\theta)$ curve.

The measurement of the angle dependence of H_{c2} in the basal plane of the tetragonal heavy-fermion superconductor is reported to have no anisotropy,[19] but in the tetragonal system, the anomalous angle dependence of H_{c2} is realized only for the d_{xz} and d_{yz} symmetry of the pair for the case of the singlet pairing. The experimental result of no anisotropy in the basal plane of the tetragonal heavy-fermion superconductor does not directly mean the s-wave pairing, since this alone cannot eliminate the possibility of the $d_{x^2-y^2}$ or $d_{3z^2-r^2}$ symmetry states. However, the possibility of the p-wave pairing is unlikely because in this case an anisotropy in the basal plane should be observed.

In several points, further investigations are possible. Our study is valid near the transition temperature because we expanded the gap equation by the small value of Δ, so extension of the theory to lower temperatures is required. The role of intersite interaction at a lower temperature may be different from that at the transition temperature.

The effect of impurities on the on-site and intersite pairing must be different. Therefore, the properties of the intersite pairing state may be modified in a different way, and this provides an insight into the role of the intersite pairing.[20]

ACKNOWLEDGMENTS

Numerical calculations were performed at the computer center of the University of Tokyo. This work was supported by a Grant-in-Aid from the Ministry of Education, Science and Culture.

*Present address: Department of Applied Physics, Faculty of Science, Science University of Tokyo, Shinjuku-ku, Tokyo 162, Japan.

[1]Y. Suwa, Y. Tanaka, and M. Tsukada, Phys. Rev. B **39**, 9113 (1989).

[2]M. Inoue, T. Takemori, K. Ohtaka, R. Yoshizaki, and T. Sakudo, J. Phys. Soc. Jpn. **56**, 3622 (1987).

[3]Zs. Gulácsi, M. Gulácsi, and I. Pop, Phys. Rev. B **37**, 2247 (1988).

[4]H. Kamimura, S. Matsuno, and R. Saito, Solid State Commun. **66**, 363 (1988).

[5]F. J. Ohkawa and H. Fukuyama, J. Phys. Soc. Jpn. **53**, 4344 (1984).

[6]K. Miyake, T. Matsuura, H. Jichu, and Y. Nagaoka, Prog. Theor. Phys. **72**, 1063 (1984).

[7]T. M. Rice, Jpn. J. Appl. Phys. **26**, Suppl. 26-3, 1865 (1987).

[8]D. Jérome and H. J. Shulz, Adv. Phys. **31**, 299 (1982).

[9]R. A. Klemm, *Electronic Properties of Inorganic Quasi-One-Dimensional Materials*, edited by P. Monceau (D. Reidel, Dordrecht, 1985), Vol. I, p. 195.

[10]C. Bourbonnais and L. G. Caron, Europhys. Lett. **5**, 209 (1988).

[11]H. Mori, J. Phys. Soc. Jpn. **58**, 1394 (1989).

[12]P. Kumar and P. Wolfle, Phys. Rev. Lett. **59**, 1954 (1987).

[13]K. Scharnberg and R. A. Klemm, Phys. Rev. B **22**, 5233 (1980).

[14]K. Scharnberg and R. A. Klemm, Phys. Rev. Lett. **54**, 2445 (1985).

[15]R. C. Morris, R. V. Coleman, and R. Bhandari, Phys. Rev. B **5**, 895 (1972).

[16]L. P. Gor'kov, Pis'ma Zh. Eksp. Teor. Fiz. **40**, 351 (1984) [JETP Lett. **40**, 1155 (1984)].

[17]K. Machida, T. Ohmi, and M. Ozaki, J. Phys. Soc. Jpn. **54**, 1552 (1985).

[18]L. I. Burlachkov, Zh. Eksp. Teor. Fiz. **89**, 1382 (1985) [Sov. Phys.—JETP **62**, 800 (1985)].

[19]V. V. Moshchalkov, F. Aliev, V. Kovachik, M. Zalyaljutdinov, T. T. M. Palstra, A. A. Menovsky, and J. A. Mydosh, J. Appl. Phys. **63**, 3414 (1988).

[20]R. A. Klemm and K. Scharnberg, Phys. Rev. B **24**, 6361 (1981).